

On Automating and Standardising Corpus Callosum Analysis in Brain MRI

Mikkel B. Stegmann and Karl Skoglund

Informatics and Mathematical Modelling, Technical University of Denmark
Richard Petersens Plads, Building 321, DK-2800 Kgs. Lyngby, Denmark
mbs@imm.dtu.dk kas@imm.dtu.dk

Abstract

Corpus callosum analysis is influenced by many factors. The effort in controlling these has previously been incomplete and scattered. This paper sketches a complete pipeline for automated corpus callosum analysis from magnetic resonance images, with focus on measurement standardisation. The presented pipeline deals with i) estimation of the mid-sagittal plane, ii) localisation and registration of the corpus callosum, iii) parameterisation and representation of its contour, and iv) means of standardising the traditional reference area measurements.

1 Introduction

Brain morphometry is an important tool for detecting and monitoring brain pathologies such as epilepsy, dementia and multiple sclerosis. A common method is to delineate some well-defined area of the brain to yield a shape for inter- or intra-subject studies. One such structure is the *corpus callosum* (CC); a white-matter nervous tissue bundle bridging the left and right cerebral hemisphere. This structure is particularly interesting due to the many neurological studies indicating relationships between the size and shape of the CC, and gender, age, handedness, neurodegenerative diseases et cetera (e.g. [9, 2, 7]). Common to such studies is that measurements are performed on the two-dimensional cross-section of the CC defined by the mid-sagittal plane (MSP), which separates the left hemisphere from the right. Possibly the most common type of CC measurement consists of partitioning the CC body into a small set of reference parts and calculating their areas. Such descriptors can subsequently be used in e.g. group studies between subjects with dementia and normal subjects.

The literature typically deals with each of these topics separately: i) estimation of the mid-sagittal

plane (e.g. [1, 8, 15]), ii) corpus callosum localisation (e.g. [9, 17, 13]), and iii) corpus callosum partitioning (e.g. [16]). To bridge these, this paper sketches a complete pipeline for automated corpus callosum analysis from magnetic resonance images (MRI) taking all of the above elements into consideration.

2 Methods

2.1 Mid-sagittal Plane Estimation

The human brain consists on a coarse level of the cerebrum, the cerebellum and the brainstem. Most prominent is the cerebrum which is divided into hemispheres connected by a nervous fibre bundle; the corpus callosum. The surface partitioning this approximate bilateral symmetry of the cerebrum is typically denoted *the mid-sagittal plane* (MSP) referring to its relative alignment with the sagittal plane of the human body. Determining the MSP is thus an invariable prerequisite for measurements on structures defined via this plane such as the MSP cross-section of the corpus callosum.

Traditionally MSP estimation is based on global symmetry which is heavily influenced by global (i.e. head) symmetry. To avoid this, we proposed an approach that optimises a local symmetry measure using the Nelder-Mead simplex method [15]; see Figure 1. The MSP is parameterized by azimuth/elevation angles and the orthogonal distance to the origin. The objective function is based on profiles normal to the plane. In addition, [15] introduced the use of thin-plate spline fitting using robust statistics for estimating a curved *mid-sagittal surface* (MSS), e.g. in pathological brains.

2.2 Corpus Callosum Localisation

Obtaining manual CC tracings is both time-consuming, error-prone and operator dependent. In-

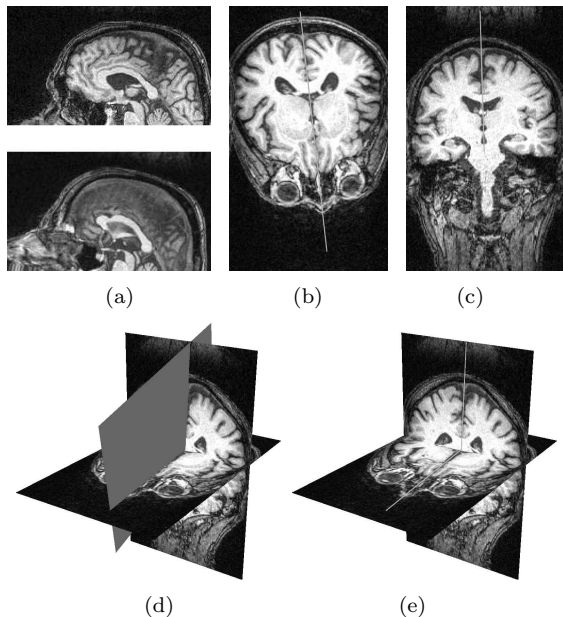


Figure 1: Automatically estimated mid-sagittal plane (MSP). (a) Initial (above) and optimal (below) MSP. (b) Axial MSP intersection. (c) Coronal MSP intersection. (d) Axial and coronal slice with estimated MSP. (e) Axial and coronal slice with MSP intersection.

stead, medical image analysis should aim at replacing this task. In [13] we introduced the use of the class of generative models; Active Appearance Models (AAMs) [4], for fully automated localisation of the CC (see Figure 2). AAMs establish a compact parameterisation of object variability, as learned from a representative training set. Objects are defined by marking up each training example with points of correspondence, i.e. landmarks. Subsequently, AAMs can be registered rapidly to unseen images. Due to their general nature and ability to deal with substantial variability, AAMs have found much use in medical applications [14].

The shape models inherent to AAMs rely on landmarks. Albeit the CC shows an apparent lack of such, papers employing shape models (e.g. using Active Shape Models [5]) have not dealt with this issue. Thus, we have based our AAMs in [13] on the concept of *minimum description length* (MDL) as introduced in [6] which led to compact and unique shape descriptors.

2.3 Representation and Analysis

While the previous sections have dealt with obtaining the CC outlines, this will touch upon an outline representation suitable for extraction of high-level features. Secondly, extraction of the traditional CC reference area measurements will be treated.

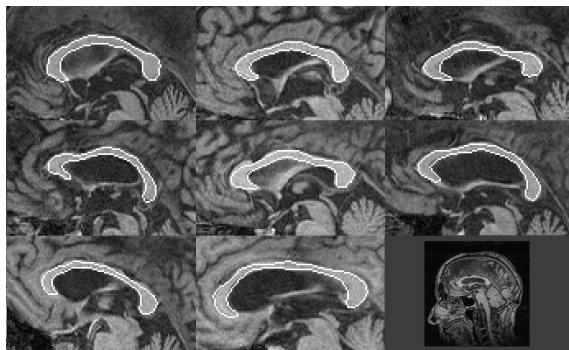


Figure 2: Automated localisation of the corpus callosum (cropped). Full MSP search slice (lower-right).

2.3.1 Fourier Representation

Closed, simple curves devoid of strong local curvature, such as the CC outline, may be represented by a Fourier series expansion. A 2D curve can be represented either as a single complex function

$$f(t) = \sum_{k=-\infty}^{k=\infty} c_k e^{ik\Omega t}, \quad (1)$$

or as separate real functions for each axis [12],

$$\begin{bmatrix} x(t) \\ y(t) \end{bmatrix} = \sum_{k=0}^{\infty} \begin{bmatrix} p_k & q_k \\ r_k & s_k \end{bmatrix} \begin{bmatrix} \cos k\Omega t \\ \sin k\Omega t \end{bmatrix}. \quad (2)$$

Here, t is the *arc-length* parameter, $\Omega = 2\pi/T$ is the *angular frequency* and T is the *period*. The coefficients c_k are calculated using *Fourier's theorem* [3]: $c_k = \frac{1}{T} \int_0^T e^{-ik\Omega t} f(t) dt$.

Usually, shapes come as delineated outlines or annotated landmarks, in which case the input function $f(t)$ is discrete. The coefficients are then found using the *discrete Fourier transform*. The N -point transform is $c_k = \frac{1}{N} \sum_{j=0}^{N-1} e^{-2\pi ijk/N} f_j$.

The Fourier representation has a number of benefits. Looking at Equation 2, an intuitive geometrical interpretation arises. $k = 0$ corresponds to a translation in the x and y directions and $k = 1$ represents a general ellipse. Indices greater than one correspond to other ellipses with increasing frequency (all are T -periodic) that modulates the main ellipse. As the elliptic components are added, the resulting shape will approximate the original data with increasing accuracy (see Figure 3).

Another benefit of the Fourier representation is the analytical nature of the shape-generating equations 1 and 2. It can be shown that a Fourier transform corresponds to a rotation in \mathbb{R}^N of the N input landmarks. This means that if all Fourier coefficients are used, no information is lost in the transformation. However, to reduce dimensionality and regularise the original data points, usually

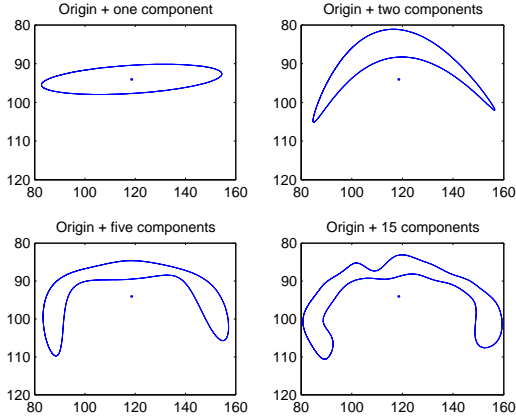


Figure 3: Fourier components of the callosal outline.

only the M first coefficients are used. Disregarding this approximation, many geometric properties and operations can be made in an exact fashion. It is e.g. simple to calculate the curvature at any position of the curve. Green’s theorem relates the boundary function to the properties of the whole enclosed area. This can be used to calculate, for instance, the area analytically.

2.3.2 Partitioning Schemes

Since no gross anatomical landmarks exist that delimit anatomically or functionally distinct callosal regions, several partitioning schemes have been devised [16]. These can be roughly divided into three categories: i) *vertical partitioning* (i.e. partitions orthogonal to a line connecting the CC “endpoints”; the rostrum and the splenium), ii) *radial partitioning* (radial sections emanating from a reference points “between” the rostrum and the splenium), iii) *curvilinear partitioning* (partitions defined by arc-length along a curvilinear reference line).

Due to the lack of landmarks, all approaches need to be defined uniquely from the contour. The first principal axis of a point-based contour representation, as shown in Figure 4, can provide such definition for category i). The centroid of the point-based contour provides a reference point for category ii). For category iii) the midpoints of chords between an arc-length sampling of the inner and outer part of the CC contour may be used [16].

Unfortunately, all of the above schemes introduce a marked shape-dependent bias of the defined callosal areas (typically five) [16]. Here we introduce two schemes designed to lessen this bias.

One solution is to use the landmarks directly from the AAM localisation due to their MDL properties. Figure 5 shows five reference areas deter-

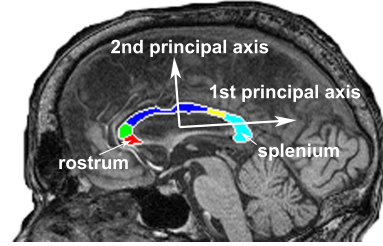


Figure 4: Principal axes and one particular set of corpus callosum reference areas.

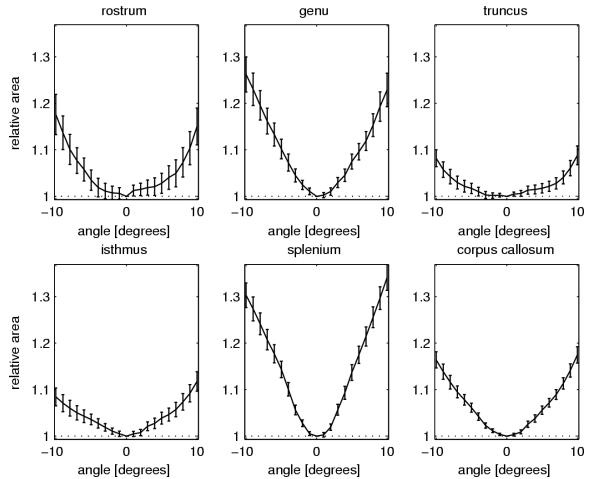


Figure 5: Mean corpus callosum area changes for varying mid-sagittal plane perturbations.

mined using this definition, as a function of MSP rotation around the 2nd principal axis of the CC. This figure also shows that accurate MSP estimation can remove potentially substantial random effects, which could be present using the typical clinical approach of employing in-scanner subject alignment only. This thereby increases the sensitivity of morphometric analyses and allow for a reduction of the number of subjects in a given population study.

Another approach is to further develop category iii) by eliminating shape-bias using an alternative definition of the curvilinear reference line. For this we employ the *chordal axis transform* [11] as a stable and convenient alternative to the *medial axis transform*. All branches of the CAT are pruned away until one axis remains, which subsequently parameterises the callosal regions. An example showing five uniform partitions of 25 corpora callosa is given in Figure 6.

3 Discussion

This paper has described the elements required to establish a complete pipeline for automated corpus

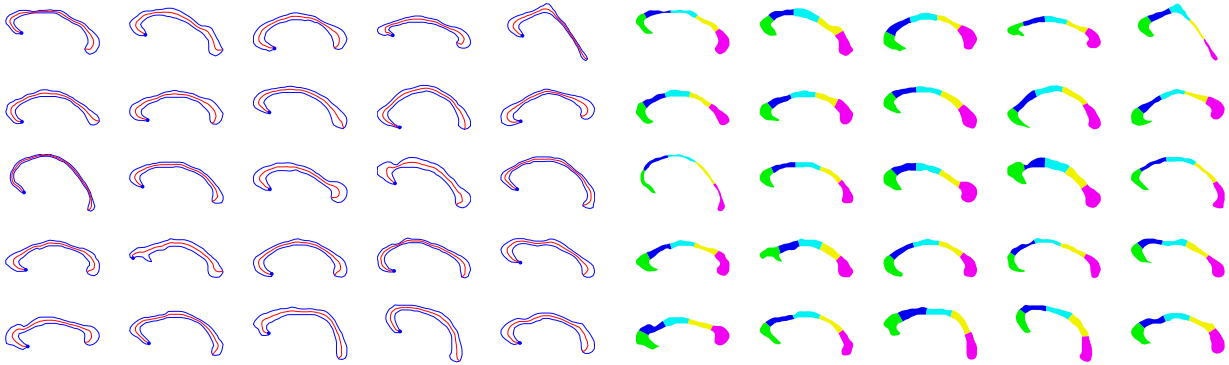


Figure 6: Corpus callosum contours and their chordal axes (left). Corresponding partitions (right).

callosus analysis; from MRIs to descriptive features. Ultimately, such a framework could be implemented in-scanner to immediately provide the required features, e.g. for large-scale data mining of callosal geometry and patient record of every scanned subject in a radiology department. Each subpart of the pipeline aims at standardising the final descriptors irrespective of the natural biological variation.

To the best of our knowledge no such system currently exists. However, based on the modules summarised here, our future work will aim at a unified system producing clinical results from the large-scale LADIS study [10] (approx. 600 subjects) in collaboration with the Danish Research Centre for Magnetic Resonance, DRCMR.

Acknowledgments

Charlotte Ryberg and Egill Rostrup, DRCMR, are gratefully acknowledged for providing MRIs. All subjects originated from a subset of the LADIS study [10]. M. B. Stegmann was supported by The Danish Medical Research Council, grant no. 52-00-0767, and The Danish Research Agency, grant no. 2059-03-0032. K. Skoglund was supported by The Technical University of Denmark, DTU.

References

- [1] B. A. Ardekani, J. Kershaw, M. Braun, and I. Kanuo. Automatic detection of the mid-sagittal plane in 3-D brain images. *IEEE Transactions on Medical Imaging*, 16(6):947–52, 1997.
- [2] F. L. Bookstein. Landmark methods for forms without landmarks: localizing group differences in outline shape. *Medical Image Analysis*, 1(3):225–244, 1997.
- [3] W. L. Briggs and Van E. Henson. *The DFT: An Owner's Manual for the Discrete Fourier Transform*. SIAM, 1995.
- [4] T. F. Cootes, G. J. Edwards, and C. J. Taylor. Active appearance models. In *Proc. of European Conf. on Computer Vision 1998*, volume 1407 of *Lecture Notes in Computer Science*, pages 484–498. Springer, 1998.
- [5] T. F. Cootes, C. J. Taylor, D. H. Cooper, and J. Graham. Active shape models – their training and application. *Computer Vision and Image Understanding*, 61(1):38–59, 1995.
- [6] R. H. Davies, C. J. Twining, T. F. Cootes, J. C. Waterton, and C. J. Taylor. A minimum description length approach to statistical shape modeling. *Medical Imaging, IEEE Transactions on*, 21(5):525–537, 2002.
- [7] A. Dubb, B. Avants, R. Gur, and J. Gee. Shape characterization of the corpus callosum in schizophrenia using template deformation. In *Medical Image Computing and Computer-Assisted Intervention - MICCAI*, volume 2, pages 381–388, 2002.
- [8] Y. Liu, R. T. Collins, and W. E. Rothfus. Robust mid-sagittal plane extraction from normal and pathological 3-D neuroradiology images. *IEEE Transactions on Medical Imaging*, 20(3):175–192, 2001.
- [9] A. Lundervold, N. Duta, T. Taxt, and A. K. Jain. Model-guided segmentation of corpus callosum in MR images. In *Computer Vision and Pattern Recognition*. IEEE Comput. Soc, 1999.
- [10] L. Pantoni, A. M. Basile, G. Pracucci, K. Asplund, J. Bogousslavsky, H. Chabriat, T. Erkinjuntti, F. Fazekas, J. M. Ferro, M. Hennerici, J. O'brien, P. Scheltens, M. C. Visser, L. O. Wahlund, G. Waldemar, A. Wallin, and D. Inzitari. Impact of age-related cerebral white matter changes on the transition to disability - the ladis study: Rationale, design and methodology. *Neuroepidemiology*, 24(1-2):51–62, 2005.
- [11] L. Prasad. Morphological analysis of shapes. *Center for Nonlinear Studies - CNLS Newsletter*, 139:1–18, July 1997.
- [12] L. H. Staib and J. S. Duncan. Boundary finding with parametrically deformable models. *Pattern Analysis and Machine Intelligence, IEEE Transactions on*, 14(11):1061–1075, 1992.
- [13] M. B. Stegmann, R. H. Davies, and C. Ryberg. Corpus callosum analysis using MDL-based sequential models of shape and appearance. In *International Symposium on Medical Imaging 2004, San Diego CA, SPIE*, pages 612–619. SPIE, feb 2004.
- [14] M. B. Stegmann, B. K. Ersbøll, and R. Larsen. FAME – a flexible appearance modelling environment. *IEEE Trans. on Medical Imaging*, 22(10):1319–1331, 2003.
- [15] M. B. Stegmann, K. Skoglund, and C. Ryberg. Mid-sagittal plane and mid-sagittal surface optimization in brain MRI using a local symmetry measure. In *International Symposium on Medical Imaging 2005, San Diego, CA, Proc. of SPIE vol. 5747*. SPIE, feb 2005.
- [16] P. M. Thompson, K. L. Narr, R. E. Blanton, and A. W. Toga. Mapping structural alterations of the corpus callosum during brain development and degeneration. In *Proceedings of the NATO ASI on the Corpus Callosum*. Kluwer Academic Press, 2001. Book Chapter in: Eran Zaidel, Marco Iacoboni [eds.].
- [17] B. van Ginneken, A. F. Frangi, J. J. Staal, B. M. Ter Haar Romeny, and M. A. Viergever. Active shape model segmentation with optimal features. *IEEE Transactions on Medical Imaging*, 21(8):924–933, 2002.